



**HAL**  
open science

## Quantitative and specific recovery of natural organic and mineral sulfur for (multi-)isotope analysis

I. Jovovic, V. Grossi, Pierre Adam, L. Simon, I. Antheaume, F. Gelin, M. Ader, P. Cartigny

### ► To cite this version:

I. Jovovic, V. Grossi, Pierre Adam, L. Simon, I. Antheaume, et al.. Quantitative and specific recovery of natural organic and mineral sulfur for (multi-)isotope analysis. *Organic Geochemistry*, 2020, 146, pp.104055. 10.1016/j.orggeochem.2020.104055 . hal-02963254

**HAL Id: hal-02963254**

**<https://hal.science/hal-02963254v1>**

Submitted on 9 Oct 2020

**HAL** is a multi-disciplinary open access archive for the deposit and dissemination of scientific research documents, whether they are published or not. The documents may come from teaching and research institutions in France or abroad, or from public or private research centers.

L'archive ouverte pluridisciplinaire **HAL**, est destinée au dépôt et à la diffusion de documents scientifiques de niveau recherche, publiés ou non, émanant des établissements d'enseignement et de recherche français ou étrangers, des laboratoires publics ou privés.

# 1 Quantitative and Specific Recovery of Natural Organic and 2 Mineral Sulfur for (Multi-)Isotope Analysis

3 I. Jovovic<sup>1\*</sup>, V. Grossi<sup>1</sup>, P. Adam<sup>2</sup>, L. Simon<sup>3</sup>, I. Antheaume<sup>1</sup>, F. Gelin<sup>4</sup>, M. Ader<sup>5</sup>, P.  
4 Cartigny<sup>5</sup>

5 <sup>1</sup>Laboratoire de Géologie de Lyon, Univ Lyon, Univ Lyon 1, ENSL, CNRS, LGL-TPE, F-  
6 69622, Villeurbanne, France

7 <sup>2</sup>Université de Strasbourg, CNRS, Institut de Chimie de Strasbourg UMR 7177, F-67000

8 Strasbourg, France<sup>3</sup>Univ Lyon, Université Claude Bernard Lyon 1, CNRS, ENTPE, UMR

9 5023 LEHNA, F-69622, Villeurbanne, France<sup>4</sup>Unconventional R&D Program, TOTAL E&P,

10 Centre Scientifique et Technique Jean Féger, 64018 Pau, France

11 <sup>5</sup>Université de Paris, Institut de physique du globe de Paris, CNRS, F-75005 Paris, France

12 \*corresponding author: [ivan.jovovic@univ-lyon1.fr](mailto:ivan.jovovic@univ-lyon1.fr)

13

## 14 ABSTRACT

15 Deciphering the role of sulfur in biogeochemical cycles strongly relies on its stable isotope  
16 composition, which ultimately depends on the ability to quantitatively recover different sulfur  
17 species from geological samples. For decades most studies have been restricted to the <sup>34</sup>S/<sup>32</sup>S  
18 composition of bulk samples, using simple methods based on the analysis of SO<sub>2</sub> released by  
19 sample combustion combined to mass spectrometry. The wet chemistry procedures required  
20 to selectively extract specific sulfur species were generally avoided due to their tediousness  
21 and inefficiency for some complex matrices, especially when targeting organic sulfur. With  
22 the recent advent of multi-isotope studies (investigating the minor sulfur stable isotopes <sup>33</sup>S  
23 and <sup>36</sup>S) which rely either on the analysis of sulfur as SF<sub>6</sub>, or on the use of secondary ion or  
24 multi-collector inductively coupled plasma mass spectrometry, wet chemistry-based

25 preparation procedures were brought back to the stage with a renewed interest in developing  
26 procedures better adapted to the investigation of specific sulfur species.

27 Here we propose a new stepwise chemical procedure for the quantitative recovery and multi-  
28 isotope analysis of organic sulfur from both solvent soluble (total lipid extract) and insoluble  
29 (kerogen) fractions, based on a wet oxidation by sodium hypochlorite. This procedure also  
30 allows the multi-isotope analysis of inorganic sulfur species (elemental sulfur, sulfates and  
31 sulfides) in the same sample. Its application to different well-known petroleum source rocks  
32 and to an oil demonstrates its relevance for disentangling the interactions between the  
33 different sulfur pools and for shedding new light on the sulfur biogeochemical cycle.

34

35 **Keywords : sulfur (multi-)isotopes; organic and mineral sulfur; source rocks; chemical**  
36 **oxidation of organic sulfur; S biogeochemical cycle**

37

## 38 1. INTRODUCTION

39 Sulfur (S) is a key element of biogeochemical cycles, being both an essential component of  
40 living cells and involved in major geological processes. The proportions of its four stable  
41 isotopes ( $^{32}\text{S}$ ,  $^{34}\text{S}$ ,  $^{33}\text{S}$ ,  $^{36}\text{S}$ , in order of natural abundance) vary upon equilibrium and/or  
42 kinetic conditions, and can be used as tracers of S biogeochemical cycles and processes  
43 (Passier et al., 1999; Canfield, 2001; Johnston, 2011). S-isotope compositions are expressed  
44 as per mil (‰) differences relative to the isotopic composition of the Vienna Canyon Diablo  
45 Troilite international standard (V-CDT), and presented in standard  $\delta$  notation:  $\delta^A\text{S} =$   
46  $^A\text{R}_{\text{sample}}/^A\text{R}_{\text{CDT}} - 1$  where  $^A\text{R} = ^A\text{S}/^{32}\text{S}$  and  $A = 33, 34$  or  $36$  (note however that there is not yet  
47 any international standard for the  $^{33}\text{S}/^{32}\text{S}$  and  $^{36}\text{S}/^{32}\text{S}$  ratios).

48 The three isotope ratios ( $\delta^{33}\text{S}$ ,  $\delta^{34}\text{S}$  and  $\delta^{36}\text{S}$ ) primarily scale on their relative mass differences  
49 and their fractionation can be predicted using an approximation of their partition function

50 (Bigeleisen and Mayer, 1947; Young et al., 2002). This is known as mass-dependent  
51 fractionation:  $\delta^{33}\text{S} \approx 0.515 \times \delta^{34}\text{S}$  and  $\delta^{36}\text{S} \approx 1.89 \times \delta^{34}\text{S}$  (see thereafter for more formal and  
52 rigorous equations). However, most studies solely focus on  $^{34}\text{S}$  fractionation, which is the  
53 easiest to measure. Such measurements have become common with the development of  
54 elemental analysis coupled to isotope ratio mass spectrometry (EA-IRMS), in which S is  
55 oxidized to  $\text{SO}_2$ , and the  $^{34}\text{SO}_2/^{32}\text{SO}_2$  ratio subsequently measured (Giesemann et al., 1994).  
56 EA-IRMS analyses of  $\delta^{34}\text{S}$  are low cost, easy and fast to operate. Though, the oxygen  
57 interferences inherent to the use of  $\text{SO}_2$  gas forbid reliable multi-isotope approaches (Rees,  
58 1978).

59 More recently, multi-isotope studies have enlightened previously poorly constrained  
60 atmospheric and (bio)(geo)chemical processes (Farquhar et al., 2000; Farquhar and Wing,  
61 2003; Luo et al., 2018). For instance, the specific  $^{32}\text{S}$ ,  $^{33}\text{S}$ ,  $^{34}\text{S}$  and  $^{36}\text{S}$  signatures of ancient  
62 rocks led to a new understanding of Archean and Paleoproterozoic atmospheric chemistry and  
63 S cycling (Farquhar et al., 2000; Philippot et al., 2007). The analysis of  $^{33}\text{S}$  and  $^{36}\text{S}$  isotope  
64 compositions was also a key factor in achieving a better understanding of hydrothermal  
65 processes (Ono et al., 2007) and microbial metabolic pathways such as sulfate reduction, S  
66 oxidation and S disproportionation (*e.g.* Farquhar et al., 2003; Johnston et al., 2005; Ono et  
67 al., 2006). The interpretations rely on both the (small) deviations in the behavior of each S-  
68 isotope and mass-conservation effects which are expressed using the conventional  $\Delta$  notation:  
69  $\Delta^{33}\text{S} = \delta^{33}\text{S} - [(\delta^{34}\text{S} + 1)^{0.515} - 1]$  and  $\Delta^{36}\text{S} = \delta^{36}\text{S} - [(\delta^{34}\text{S} + 1)^{1.89} - 1]$ . As for any isotope  
70 method, the determination of the multi-isotope composition of specific S species in a given  
71 sample (*e.g.* sulfates, sulfides, elemental sulfur ( $\text{S}^0$ ), organic sulfur; Table 1) requires the  
72 quantitative recovery and purification of the different S pools. Sulfides (and/or acid volatile  
73 S), sulfates and  $\text{S}^0$  are typically recovered as  $\text{Ag}_2\text{S}$  using distillation methods and reducing  
74 solutions (Thode et al., 1958; Pepkowitz and Shirley, 1950; Forrest and Newman, 1977;

75 Canfield et al., 1986). Each targeted S-pool is first converted into H<sub>2</sub>S by an adapted acid  
76 treatment, and subsequently recovered as a solid metal sulfide (typically as Ag<sub>2</sub>S, sometimes  
77 as ZnS or CdS). The obtained metal sulfide is then transformed into either SO<sub>2</sub> or SF<sub>6</sub> (e.g.  
78 Thode et al., 1961; Thode and Rees, 1971, respectively) and analyzed by IRMS. Contrary to  
79 oxygen, fluorine has only one stable isotope. Because it avoids the need for <sup>17</sup>O or <sup>18</sup>O  
80 corrections (Rees, 1978), IRMS analysis of SF<sub>6</sub> is more precise and accurate and, accordingly,  
81 has been preferentially used to investigate all four S stable isotopes (Hulston and Thode,  
82 1965). This, however, requires a non-automated conversion of Ag<sub>2</sub>S into gaseous SF<sub>6</sub> and the  
83 purification of the latter. Alternatively, the use of secondary ion mass spectrometry (SIMS)  
84 has been proposed for the *in-situ* analysis of <sup>32</sup>S, <sup>33</sup>S and <sup>34</sup>S (e.g. Thomassot et al., 2009;  
85 Whitehouse, 2012), and multi-collector inductively coupled mass spectrometry (MC-ICPMS)  
86 has been used for the determination of <sup>32</sup>S, <sup>33</sup>S and <sup>34</sup>S contents in small purified samples (e.g.  
87 Albalat et al., 2016). SIMS is however less available and requires specific standards. Though  
88 high precision measurements of <sup>34</sup>S can be obtained with MC-ICPMS (e.g. Paris et al., 2013),  
89 this technique is hardly as precise as IRMS analysis of SF<sub>6</sub> for <sup>33</sup>S-measurements and cannot  
90 provide <sup>36</sup>S data.

91 Organic sulfur (S<sub>org</sub>) is, after pyrite, the second most abundant reduced S pool in sediments  
92 (Anderson and Pratt, 1995), where it usually occurs as a complex mixture of monomeric and  
93 polymeric organosulfur compounds (OSC). Sedimentary S<sub>org</sub> can be further divided into a  
94 soluble (solvent-extractable) and an insoluble (non-extractable or residual) OSC-pools.  
95 Biosynthetic S<sub>org</sub> mainly occurs as chemically labile proteins and amino acids that are  
96 expected to be quickly degraded during diagenesis (Tissot and Welte, 1984 ; Kutuzov et al.,  
97 2019) though, in some cases, they could contribute their sulfur atoms to the kerogens (Raven  
98 et al., 2018). On the other hand, S<sub>org</sub> in recent sediments typically increases with depth. For  
99 example, Werne et al. (2003) showed an increase from 0.05 to 0.12 of the organic S/C ratio in

100 the Cariaco Basin with sediment depth. This increase reflects a diagenetic S-enrichment of  
101 organic matter by sulfurization processes (natural vulcanization) which involve reduced S  
102 species produced by microbial sulfate reduction (MSR; Sinninghe Damsté et al., 1989; Adam  
103 et al., 1993). The idea of a common source of sedimentary  $S_{\text{org}}$  and mineral S (usually pyrite)  
104 is further supported by their respective  $\delta^{34}\text{S}$  signatures generally depleted relative to sulfates  
105 (*e.g.* Thode et al., 1958; Zaback and Pratt, 1992; Tuttle and Goldhaber, 1993; Canfield et al.,  
106 1998; Werne et al., 2003). However,  $S_{\text{org}}$  is still often  $^{34}\text{S}$ -enriched relative to pyrite (*e.g.* 10-  
107 20‰ in marine sediments, Orr, 1986; 5-8‰ in Cariaco Basin, Werne et al., 2003). Tuttle  
108 (1991), then Werne et al. (2003) explained this relative enrichment by a delayed sulfurization  
109 of organic matter relative to the formation of pyrite, but this simple view likely overlooks the  
110 fact that different organic molecules may react with reduced species at different rates  
111 depending on the context (*e.g.* Amrani, 2014, Raven et al., 2016a, Raven et al., 2016b,  
112 Shavar et al., 2020).

113 Thus, our understanding of the biogeochemical S cycle still remains incomplete and could  
114 clearly benefit from  $S_{\text{org}}$  multi-isotope analyses, but only few dedicated studies have been  
115 performed so far (*e.g.* Oduro et al., 2011, Labidi et al., 2017, Siedenberg et al., 2018).  
116 Reasons are linked to the structural diversity and distinct solubilities of biological and  
117 geological OSC, and to their difficult clear-cut separation from the inorganic S pools, which  
118 make them more arduous to recover specifically and quantitatively. In this respect, an adapted  
119 procedure for the specific and quantitative recovery of  $S_{\text{org}}$  would also be useful for studies  
120 dedicated to  $^{34}\text{S}_{\text{org}}$  signatures. Most existing procedures for the release of  $S_{\text{org}}$  rely on its  
121 oxidation into sulfates by combustion methods such as Eschka fusion (using a 2:1 mixture of  
122  $\text{MgO}$  and  $\text{Na}_2\text{CO}_3$  at *ca.* 900°C, Eschka, 1874), or  $\text{Na}_2\text{O}_2$  Parr bomb and  $\text{Br}_2$  oxidations, with  
123 yields close to 100% and a good replicability (Selvig and Fieldner, 1927; Siedenberg et al.,

124 2018). However, those methods are tedious, dangerous and difficult to apply routinely to large  
125 sets of samples.

126 More recently, some studies have introduced the use of specific methods to improve  $S_{\text{org}}$   
127 recovery for (multiple) S-isotope measurements (Table 1). For instance, Oduro et al. (2011)  
128 used Raney nickel as a catalyst for the desulfurization of volatile OSC and the recovery of  $S_{\text{org}}$   
129 as nickel sulfide. Though they showed yields close to 100% for the desulfurization of many  
130 volatile OSC, this method did not appear suitable for the recovery of sulfones. Moreover,  
131 Raney nickel is a solid which poorly reacts with insoluble OSC from kerogens. To our  
132 knowledge, none of the presently available procedures allows a simple, selective and  
133 quantitative recovery of both mineral S and  $S_{\text{org}}$  pools.

134 Here we propose a new stepwise chemical procedure for the selective and quantitative  
135 recovery as  $\text{Ag}_2\text{S}$  of solvent-extractable and non-extractable  $S_{\text{org}}$  from sediments and oils,  
136 applicable for a specific and reliable determination of either  $^{34}\text{S}$  or the multiple S-isotope  
137 composition of distinct  $S_{\text{org}}$  pools. It relies on oxidation of organic matter with sodium  
138 hypochlorite ( $\text{NaOCl}$ ), which was previously shown to release organic-bound S as sulfates  
139 (*e.g.* Li and Cho, 2005). This procedure is further compatible with the analysis of sulfides,  
140 sulfates and  $\text{S}^0$  in the same samples. The complete optimized procedure was carefully tested  
141 on an oil and sediment samples from lacustrine and marine environments of various ages  
142 (from modern to 50 Myr), validating its suitability for the (multi-)isotope analysis of  
143 geological organic and mineral S and allowing a new model of the S cycle to be considered  
144 for some depositional environments.

145

## 146 **2. MATERIAL AND METHODS**

### 147 **2.1. Samples**

148 Due to the large diversity of S forms in nature, their distinct reactivity and potential  
149 interaction with natural matrices, our method was developed and tested on several natural  
150 samples rather than pure minerals and OSC. These samples were selected among organic  
151 matter- and S-rich sediment formations from various locations, and complemented with a S-  
152 rich oil (Table 2).

153 We selected sediments from the Eocene Green River Fm Mahogany Zone (Utah, USA,  
154 Bradley, 1964; Smith and Carroll, 2015; Tuttle, 1991), and sub-superficial sediments from the  
155 modern Lake Dziani Dzaha (Mayotte, Indian Ocean, Leboulanger et al., 2017; Milesi et al.,  
156 2020). A marine shale sample from the Miocene Monterey Fm (California, USA, Orr, 1986;  
157 Zaback and Pratt, 1992) was added to the sample set. Lastly, we used a sample from Rozel  
158 Point seeps (Utah, USA, Thode et al., 1958; Eardley, 1963; Mauger et al., 1973) to evaluate  
159 the efficiency of the new method on pure organic matter. A non-referenced sample from the  
160 Limagne Basin (Massif Central, France, Wattinne et al., 2003; Seard et al., 2013) was added  
161 to compare the yields of  $S_{org}$  obtained with Raney nickel (Oduro et al., 2011) and the newly  
162 developed method (Table 3).

163 None of these samples was thermally mature except for the Rozel Point oil seep sample for  
164 which maturity was hardly defined (Eardley, 1963); thermal maturation effects on  $S_{org}$   
165 recovery is therefore not discussed in this study.

166

## 167 **2.2. Analytical steps**

168 Samples were freeze dried, ground to  $<100\ \mu\text{m}$ , and homogenized. Subsamples (*ca.* 1 g) were  
169 then subjected to a sequence of chemical extractions in order to specifically recover the  
170 different organic (soluble and insoluble) and mineral ( $S^0$ , sulfates, sulfides) S pools (Fig. 1).

171 Only Pyrex glassware was used and all chemicals were reagent-grade. Dilutions and washes  
172 were performed in 100 mL centrifuge tubes using deionized water. S-purity of all reagents



173 was regularly checked and considered as acceptable when less than 5 µg of S was recovered  
174 in a whole blank procedure.

175

#### 176 2.2.1. *Solvent extraction and S<sup>0</sup> precipitation*

177 The soluble organic matter was extracted by multiple sonication cycles (10 minutes each)  
178 with methanol (MeOH, twice), dichloromethane (DCM):MeOH (1:1, v/v, twice) and DCM  
179 (twice) at room temperature (*ca.* 20°C). The total lipid extract (TLE) was treated with  
180 activated copper curls to precipitate S<sup>0</sup> as Cu<sub>x</sub>S<sub>y</sub> (Blumer, 1957).

181

#### 182 2.2.2. *Reducing distillations*

183 The acidic CrCl<sub>2</sub> (Canfield et al., 1986) and STRIP (Forrest and Newman, 1977; Pepkowitz  
184 and Shirley, 1950; Thode et al., 1961) solutions have been extensively used for the extraction  
185 of mineral S compounds in samples from a wide range of natural settings and laboratory  
186 experiments. Gröger et al. (2009) have shown that the CrCl<sub>2</sub> solution typically converts 99±1  
187 % of both sulfides and S<sup>0</sup> into H<sub>2</sub>S, but hardly reacts with individual OSC and sulfates  
188 (typical yields <0.2 %). However, since the reactivity of the CrCl<sub>2</sub> solution has never been  
189 tested against very fresh natural OM, the eventuality of a reaction with some OSC, *e.g.*  
190 organic polysulfides cannot be totally excluded. Moreover, Arnold et al. (2014) have shown  
191 that the STRIP solution typically yields close to 100 % of both sulfides and sulfates, but  
192 hardly converts OSC to H<sub>2</sub>S. Therefore, the CrCl<sub>2</sub> solution was used to selectively recover  
193 sulfide-S and Cu<sub>x</sub>S<sub>y</sub>-S, whereas the STRIP solution was used to recover sulfate-S from  
194 sulfide-free samples.

195 Due to its sensitivity towards oxidation, the CrCl<sub>2</sub> solution was prepared daily according to  
196 Fossing and Jorgensen (1989). A glass bottle closed with a teflon-coated rubber cap was filled  
197 with a an acidic CrCl<sub>3</sub> solution (80 ml of 3 % HCl and 21.15 g CrCl<sub>3</sub>, 6 H<sub>2</sub>O). The Cr(III)

198 solution was then reduced to Cr(II) by the addition of zinc granules (14 g). The solution was  
199 stirred under a nitrogen flush until the initial dark green color had completely turned to bright  
200 blue.

201 The STRIP solution is more stable and was used within 6 months after preparation. A glass  
202 Erlenmeyer flask was filled with 523 ml of 37 % HCl, 321 ml of 57 % hydriodic acid (HI)  
203 and 156 ml of 50 % hypophosphorous acid (H<sub>3</sub>PO<sub>2</sub>). The solution was heated under a nitrogen  
204 flush and gently refluxed, for 6 hours.

205 The apparatus that was used for S distillation is represented in Fig. 2. We ensured that the  
206 treated sample did not contain more than *ca.* 125 μmol S to guarantee a large excess of  
207 reagents and allow the reaction to be quantitative. The targeted S pool was converted to H<sub>2</sub>S  
208 with either 10 mL of 37 % HCl and 25 mL of CrCl<sub>2</sub> solution (sulfides/S<sup>0</sup>) or 25 mL of STRIP  
209 solution (sulfates), and refluxed for 3 hours. Produced H<sub>2</sub>S was purged and precipitated as  
210 Ag<sub>2</sub>S in a silver nitrate trap (20 ml of 2.48 % AgNO<sub>3</sub>). A few drops of a 25 % ammonia  
211 solution were added to the the Ag<sub>2</sub>S precipitate, which was then centrifuged, washed three  
212 times with 30 ml of deionized water, and lyophilized. The dry Ag<sub>2</sub>S powder was stored out of  
213 sunlight before fluorination and S multi-isotope analysis.

214

### 215 2.2.3. *Oxidation of organic matter*

216 The mineral S-free sediments/oils and S<sup>0</sup>-free TLE were heated at 60 °C under stirring with a  
217 10-15 % NaOCl solution in a 100 mL centrifuge Pyrex tube. It is noteworthy that, even under  
218 reflux and stirring, concentrated NaOCl easily tends to evaporate, resulting in a poor  
219 reactivity, especially over long reaction times. Therefore, the solution was kept under 70 °C.  
220 To guarantee a large excess of hypochlorite ions, we introduced no more than *ca.* 125 μmol S  
221 and *ca.* 25 mmol C from each sample for 25 ml of NaOCl solution. Various treatment times  
222 (6, 12, 24 and 48 hours) were tested to evaluate the reaction kinetics. This oxidative digestion

223 of organic matter resulted in the liberation of  $S_{\text{org}}$  from solvent-soluble or insoluble organic  
224 matter as sulfates. After reaction, the solution was carefully acidified with 37 % HCl, until pH  
225 <2, to allow the consumption of excess hypochlorite ions and carbonate by-products, and to  
226 facilitate the precipitation of sulfates. Sulfates were precipitated as  $\text{BaSO}_4$  using 20 mL of a  
227 saturated  $\text{BaCl}_2$  solution ( $>360 \text{ g.L}^{-1}$ ). The resulting precipitate was centrifuged and rinsed  
228 twice with 20 mL of the saturated  $\text{BaCl}_2$  solution, than freeze dried and homogenized before  
229 distillation as illustrated in 2.2.2.

230

#### 231 2.2.4. TOC and GC-MS analyses

232 The evolution of total organic carbon (TOC) contents in residual sediments during digestion  
233 was monitored using an elemental analyzer (Vario ISOTOPE Select, Elementar) equipped  
234 with a Thermal Conductivity Detector. The accuracy of the measurements was evaluated  
235 using an international sediment standard, namely IVA33802151 (TOC = 9.15 %).

236 Residual aqueous phases after oxidation with NaOCl were extracted with DCM and ethyl  
237 acetate, successively, to investigate the potential soluble organic compounds freed by the  
238 process. The extracts were then derivatized with diazomethane and analyzed by gas  
239 chromatography coupled to mass spectrometry (GC-MS), using a Thermo Trace gas  
240 chromatograph coupled to a Thermo TSQ Quantum mass spectrometer operating in the  
241 electron ionization mode (70 eV) and scanning  $m/z$  50 to 700. The temperature of the source  
242 was set to 220 °C. Gas chromatographic separations were performed on a HP5-MS column  
243 (30 m length with 0.25 mm diameter and 0.1 $\mu\text{m}$  film thickness) with helium as carrier gas  
244 (1.1  $\text{mL.min}^{-1}$ ). The temperature program was: 40°C (10 min), 40-300 °C (6 °C.min $^{-1}$ ),  
245 isothermal at 300 °C (25 min).

246

#### 247 2.2.5. Isotope analyses

248 The Ag<sub>2</sub>S powders corresponding to the different organic and mineral S pools were freeze  
249 dried, homogenized and weighed in aluminum boats before being fluorinated overnight in  
250 Nickel bombs with excess fluorine gas at 350°C. The produced SF<sub>6</sub> was purified  
251 cryogenically and by subsequent gas chromatography prior to the determination of its δ<sup>33</sup>S,  
252 δ<sup>34</sup>S and δ<sup>36</sup>S values using a Thermo Scientific MAT 253 dual-inlet IRMS (Au Yang et al.,  
253 2016). The accuracy of the measurements was evaluated using an international Ag<sub>2</sub>S standard,  
254 namely IAEA-S1 (also known as Vienna-CDT), with a δ<sup>34</sup>S value = -0.3 ‰. Typical  
255 analytical deviations were below 0.01 ‰ and 0.1 ‰ for δ<sup>33</sup>S or δ<sup>34</sup>S and δ<sup>36</sup>S values,  
256 respectively, and ≈ 0.005 ‰ and 0.1 ‰ for Δ<sup>33</sup>S and Δ<sup>36</sup>S values, respectively (1σ).

257 Total sulfur contents (TS) and associated δ<sup>34</sup>S values were measured with a VarioPYROcube  
258 elemental analyzer (Elementar) in NCS combustion mode interfaced in continuous-flow mode  
259 with an Isoprime 100 IRMS (Fourel et al., 2014). The accuracy of those measurements was  
260 evaluated using the aforementioned international Ag<sub>2</sub>S standard and one international BaSO<sub>4</sub>  
261 standard (NBS-127, δ<sup>34</sup>S value = +20.3 ‰). Typical analytical deviations were below 0.05 %  
262 and 0.3 ‰ for the TS and δ<sup>34</sup>S values, respectively (1σ).

263

### 264 **3. RESULTS AND DISCUSSION**

#### 265 **3.1. Procedure validation**

266 Subsamples were first used to test and optimize the oxidation procedure of S<sub>org</sub> with NaOCl.  
267 Then, triplicates of most samples were treated with the full stepwise procedure (Fig. 1 and  
268 Table 2). Using a mass balance calculation, the results of the triplicate analyses were  
269 compared to those obtained by direct EA-IRMS analysis of the dry sediments as a quantitative  
270 validation of the overall analytical workflow.

271

##### 272 *3.1.1. S<sub>org</sub> oxidation to sulfates and recovery*

273 Figure 3 shows the evolution of the carbon- and sulfate-contents in TLE and mineral-S free  
274 kerogens during 48 hours of NaOCl oxidation at 60°C. Within 24 hours, less than  $7 \pm 3$  % of  
275 the initial carbon remained in the sample, and more than  $95 \pm 5$  % of  $S_{org}$  was recovered as  
276 sulfates. The GC-MS analysis of residual organic compounds in aqueous phases after 4 and  
277 12 hours of oxidation showed the occurrence of carboxylic diacids (> 4 carbons), chlorinated  
278 carboxylic monoacids as well as chlorinated and non-chlorinated benzene carboxylic  
279 polyacids (up to hexa-acids). Those products are expectable during the oxidation of organic  
280 matter with NaOCl (Wang et al., 2014). More importantly, no OSC (*e.g.* thiols, thiophenes,  
281 sulfoxides, sulfones, sulfonic acids, thioesters, polysulfides) was identified in any aqueous  
282 phase, showing an efficient oxidation of S bound to organic matter into recoverable sulfates.  
283 It cannot be excluded, however, that some OSC in other matrixes may react less efficiently,  
284 thus requiring a longer reaction time to be entirely oxidized.

285 The remaining  $S_{org}$  recovered after 6, 12, 24 and 48 hours revealed no significant isotope  
286 evolution associated with the oxidation process (Fig. 4). This suggests that the progressive  
287 organic matter digestion is not associated with significant isotope effects, and that an  
288 incomplete oxidation of  $S_{org}$  in samples would not impact S isotopes measurement –though  
289 quantitative aspects should not be considered in this case.

290 For some samples, the yield of  $S_{org}$  obtained with our new method was compared with that  
291 obtained with the Raney nickel desulfurization method used by Oduro et al. (2011). Much  
292 higher yields were obtained with the new method for soluble  $S_{org}$  (7 to 200 times, Table 3),  
293 which can be explained by a possible high steric hindrance of  $S_{org}$  in these specific samples.  
294 Unsurprisingly, due to the low kinetics of unfavorable solid-solid reactions, the new method  
295 was also significantly more efficient for the insoluble  $S_{org}$  present in kerogens, compared with  
296 the 4-times lower recovery of this S pool using Raney nickel (Table 3). None of the quantities

297 of  $S_{\text{org}}$  recovered with Raney nickel were sufficient for the determination of S isotopic  
298 composition with Fluorination-IRMS.

299

### 300 *3.1.2. Mass balance validation*

301 The TS content and bulk  $\delta^{34}\text{S}$  value measured for each bulk sample were compared to those  
302 calculated from the S multi-pool analysis of the same sample (triplicate analyses), using the  
303 following mass balance equation :  $\%S_{\text{total}} \times \delta^{34}\text{S}_{\text{total}} = \Sigma(\%S_i \times \delta^{34}\text{S}_i)$ , where  $i$  is in {soluble  
304  $S_{\text{org}}$ , insoluble  $S_{\text{org}}$ ,  $S^0$ , sulfides, sulfates}.

305 The results are presented in Figure 5. The very good consistency between the two approaches  
306 ( $\text{RMSE}_{\text{TS}} = 0.13\%$  and  $\text{RMSE}_{\delta^{34}\text{S}} = 1.07\text{‰}$ ) and the good replicability of the new method (as  
307 shown by the error bars) demonstrate that this new method indeed allows the reliable and  
308 quantitative recovery of both soluble and insoluble  $S_{\text{org}}$ .

309

### 310 *3.1.3. Suitability for multi-isotopes analyses*

311 In addition to the selective and quantitative recovery of different mineral (sulfates, sulfides  
312 and  $S^0$ ) and organic (solvent-extractable and non-extractable) S pools, the new stepwise  
313 procedure developed allows the reliable determination of their S (multi-)isotope composition  
314 by IRMS ( $^{32}\text{S}$ ,  $^{33}\text{S}$ ,  $^{34}\text{S}$ ,  $^{36}\text{S}$ ) or MC-ICPMS ( $^{32}\text{S}$ ,  $^{33}\text{S}$ ,  $^{34}\text{S}$ ). In the present case, the S multi-  
315 isotope composition of the investigated samples (from IRMS analysis of  $\text{SF}_6$  gas) showed  
316 mass-dependent fractionation of all S-isotopes with small but significant  $\Delta^{33}\text{S}$  and  $\Delta^{36}\text{S}$   
317 values, within the range of  $\Delta^{33}\text{S} \approx \pm 0.10\text{‰}$  and  $\Delta^{36}\text{S} \approx \pm 1.50\text{‰}$  (Fig. 6 and Table 4) that are  
318 expected for sediments younger than 2 Ga (see review by Johnston, 2011).

319

### 320 *3.1.4. Suitability for pure organic substrates*

321 The Rozel Point oil was primarily used here to test our oxidation procedure on ‘pure’ S-rich  
322 (> 90 mg S/g oil) organic matter. The  $^{34}\text{S}$  composition of soluble  $\text{S}_{\text{org}}$  as obtained from the  
323 new method ( $\delta^{34}\text{S} = -6.05 \pm 0.11 \text{ ‰}$ , Table 4) differed by  $\approx 1.5 \text{ ‰}$  from the EA-IRMS  
324 measurement ( $\delta^{34}\text{S} = -7.5 \pm 0.3 \text{ ‰}$ ). Still, most of  $\text{S}_{\text{org}}$  could be recovered with the new method  
325 (with TS estimated to  $9.18 \pm 0.1 \text{ ‰}$  against  $9.29 \pm 0.2 \text{ ‰}$  with EA-IRMS), supporting the  
326 applicability of our procedure to ‘pure’ petroleum mixtures of OSC (possibly with a longer  
327 reaction time).

328 Yet, the efficiency of the method on fresh biological OSC and on very mature OSC (*e.g.*,  
329 Precambrian organic matter) remains to be established but should not be problematic.

330

### 331 **3.2. Comparison with literature data and further interpretation of the geological** 332 **record**

333 Though the source rocks considered in this study have already been largely studied, the S  
334 stable (multi-)isotope composition of their different S pools remains poorly documented. A  
335 comparison between our  $^{34}\text{S}$  data and those reported in previous studies of the Monterey and  
336 the Green River Formations is illustrated in Figure 7. This is complemented by data obtained  
337 for the present-day Lake Dziani Dzaha. Our multi-pool and multiple S-isotope data (Table 4),  
338 although still limited, were further used to bring new insights on our present understanding of  
339 the S isotope signatures observed in these settings (Fig. 8).

340

#### 341 *3.2.1. Monterey Formation*

342 The investigated sample of the Monterey Fm mainly contained sulfides and insoluble  $\text{S}_{\text{org}}$   
343 ( $4.73 \pm 0.30$  and  $3.57 \pm 0.22 \text{ mg/g}$  of dry sediment, respectively; Table 4). Sulfates and soluble  
344  $\text{S}_{\text{org}}$  were also present but their concentrations were *ca.* ten times lower than those of sulfides  
345 and insoluble  $\text{S}_{\text{org}}$ , respectively (Table 4).  $\text{S}^0$  was not detected, in accordance with the

346 literature (Zaback and Pratt, 1992). The presence of sulfates (which are only 2-4 ‰  $^{34}\text{S}$ -  
347 enriched relative to sulfides; Table 4) was not described as primary in previous literature and  
348 could either correspond to artifactual oxidation products formed after sampling (likely during  
349 transport and storage) from sulfide minerals and potential organic polysulfides, or to  
350 secondary gypsum possibly derived from oxidation of S associated to migrating hydrocarbons  
351 (personal communication A.L. Sessions). Sulfides appeared 3-5 ‰ depleted in  $^{34}\text{S}$  ( $\delta^{34}\text{S} =$   
352  $+2.79 \pm 0.61$  ‰) relative to soluble ( $\delta^{34}\text{S} = +6.01 \pm 0.20$  ‰) and insoluble ( $\delta^{34}\text{S} = +8.73 \pm 0.04$   
353 ‰)  $\text{S}_{\text{org}}$ . This is consistent with literature data (Zaback & Pratt, 1992, Fig. 5) and with  
354 classical biogeochemical models of the S cycle in ‘open’ sedimentary systems (Fig. 8a).  
355 Indeed, despite a large heterogeneity of sedimentary facies in the Monterey Fm, most of them  
356 are described as marine-influenced deposits (Orr, 1986; Zaback and Pratt, 1992). In these  
357 environments, S mainly derives from marine sulfates ( $\delta^{34}\text{S} \approx +20$  ‰) which, in anoxic  
358 porewaters, can be reduced to  $\text{H}_2\text{S}$  by MSR (Canfield and Des Marais, 1993). This major  
359 microbial process is associated with a large depletion in  $^{34}\text{S}$ , typically with  $\delta^{34}\text{S}_{\text{porewater sulfate}} -$   
360  $\delta^{34}\text{S}_{\text{H}_2\text{S}} = 30$  to  $50$  ‰ (Habicht and Canfield, 1997; Canfield, 2001).  $^{34}\text{S}$ -depleted  $\text{H}_2\text{S}$  can  
361 then react with sedimentary iron or organic matter to produce iron sulfides or OSC,  
362 respectively. While the formation of iron sulfides only induces small S isotope fractionations,  
363 the sulfurization of organic matter seems to induce a slight  $^{34}\text{S}$ -enrichment (generally  $< 5$  ‰)  
364 of  $\text{S}_{\text{org}}$  relative to sulfides (Orr, 1986; Werne et al., 2003; Amrani, 2014). This is classically  
365 explained by a different timing of sulfurization, with the formation of iron sulfides (classically  
366 pyrite) occurring faster than the sulfurization of organic matter (Tuttle, 1991; Tuttle and  
367 Goldhaber, 1993; Werne et al., 2003). As schematized in Figure 8a, the delayed sulfurization  
368 of organic matter likely involves sulfates/reduced sulfur species enriched in  $^{34}\text{S}$  by Rayleigh  
369 fractionation of the residual inorganic S pool. With time, this may result in a continuous  
370 enrichment of the  $\delta^{34}\text{S}$  signatures of sulfides and  $\text{S}_{\text{org}}$  until the source of mineral S is totally



371 depleted (Thode et al., 1961; Zaback and Pratt, 1992; Tuttle and Goldhaber, 1993; Fig 8a), as  
372 supported by the large range of  $\delta^{34}\text{S}$  values of sulfides (between  $\approx -9$  ‰ and  $\approx +20$  ‰)  
373 reported for the Monterey Fm (Fig. 7; Zaback and Pratt, 1992). However, upon Rayleigh  
374 fractionation, one would predict positive  $\Delta^{33}\text{S}$  ( $> 0.1$  ‰) and strongly negative  $\Delta^{36}\text{S}$  ( $< 1.0$  ‰)  
375 (see Ono et al., 2006b; Sansjofre et al., 2016) which would result from mass-conservation  
376 effects (e.g. Farquhar et al., 2007). These values are however not observed in the present  
377 study, which deserves further investigation with a larger set of samples.

378

### 379 3.2.2. *Green River Fm and Lake Dziani Dzaha*

380 As for the Monterey Fm, the main S pools in the selected samples from the Mahogany Zone  
381 of the Green River Fm and from the sub-surface sediments of Lake Dziani Dzaha were  
382 sulfides and  $\text{S}_{\text{org}}$  (Table 4). This latter, however, essentially occurred as solvent insoluble  $\text{S}_{\text{org}}$   
383 in Lake Dziani Dzaha ( $0.34 \pm 0.05$  and  $3.69 \pm 0.18$  mg/g of dry sediment for soluble and  
384 insoluble  $\text{S}_{\text{org}}$ , respectively), whereas the amount of soluble  $\text{S}_{\text{org}}$  in the sample from the Green  
385 River Fm was of the same order of magnitude as insoluble  $\text{S}_{\text{org}}$  ( $2.32 \pm 0.02$  and  $3.79 \pm 0.25$   
386 mg/g of dry sediment, respectively). Sulfides (essentially iron sulfides) were also present in a  
387 *ca.* four times higher concentration in the Green River Fm than in Lake Dziani. Variable  
388 relative abundances of the main S pools between both samples might reflect varying organic  
389 matter source or nature, sulfurization mechanisms, iron availability and depositional and  
390 diagenetic (e.g., ageing) histories (Table 2). A significant amount of  $\text{S}^0$  ( $0.66 \pm 0.04$  mg/g of  
391 dry sediment) was also detected in Lake Dziani Dzaha sediments while only traces ( $< 0.005$   
392 mg/g of dry sediment) were detected in the Green River sample. Low amounts of sulfates ( $<$   
393 5.5 % of total S) were recovered in both samples, which likely are artifactual oxidation  
394 products of mineral sulfides and eventual organic polysulfides. A strong argument for the  
395 absence of native sulfates in sediments from Lake Dziani Dzaha is the very low content of

396 sulfates ( $< 3 \mu\text{M}$ ) in the present-day partially anoxic water column (Leboulanger et al., 2017)  
397 which is far from their supersaturation threshold. Despite differences in S content and  
398 speciation, the selected samples from the Green River Fm and from Lake Dziani showed  
399 striking similarities in their S multi-isotope compositions (Table 4 and Figure 7), with sulfides  
400 exceptionally enriched in heaviest S-isotopes (*i.e.*,  $\delta^{34}\text{S} \approx +35 \text{‰}$ ), while solvent soluble and  
401 insoluble  $\text{S}_{\text{org}}$  being strongly depleted (by -25 to -30 ‰ for  $^{34}\text{S}$ ) relative to sulfides (Table 4).  
402 Highly- $^{33}\text{S}$ ,  $^{34}\text{S}$  and  $^{36}\text{S}$ -enriched  $\text{S}^0$  was also observed in Lake Dziani Dzaha with values of  
403  $\delta^{34}\text{S}$ ,  $\delta^{33}\text{S}$  and  $\delta^{36}\text{S}$  slightly above those of sulfides ( $\approx +4$ ,  $+2$  and  $+7 \text{‰}$ , respectively, *i.e.*  $\approx$   
404  $+5.5 \%$  of their values). Such uncommon S isotope features suggest strong similarities  
405 between these two ecosystems and a biogeochemical functioning clearly distinct from that of  
406 marine systems such as the Monterey Fm (Figs. 7 and 8).  
407  $^{34}\text{S}$  highly-enriched sulfides have already been reported in samples from the late stages of the  
408 Green River Fm (Thode et al., 1958; Mauger et al., 1973; Tuttle and Goldhaber, 1993). The  
409 authors suggested that this enrichment was the result of a long-term Rayleigh fractionation  
410 process in past Green River lakes, driven by MSR and the diagenetic precipitation of depleted  
411 sulfides. According to Tuttle and Goldhaber (1993), a main difference with ‘open’ marine  
412 systems is that Green River lakes behaved as ‘closed’ systems, *i.e.* with no renewing of  
413 sulfate from the water column. Lake Dziani Dzaha can actually be considered similarly. This  
414 hypersaline tropical and insular stratified phreatomagmatic crater lake has no present-day  
415 connection to seawater, but its high S content most likely originates from initial marine  
416 sulfates (Leboulanger et al., 2017). In such ‘closed’ and stratified systems, the presence of a  
417 large anoxic water layer favors the production of sulfides by MSR and their subsequent  
418 precipitation as iron sulfides or their reaction with of organic matter, inducing a progressive  
419 enrichment in heavy isotopes of the residual S pool (Fig. 8b). It is noteworthy, however, that  
420 the geological record of the Green River Fm is the result of multiple long-scale sedimentary

421 evolutions over 100,000 years (Tuttle and Goldhaber, 1993), whereas the sedimentary story of  
422 Lake Dziani Dzaha is less than 9000 years (Zinke et al., 2003). Different mechanisms could  
423 have been involved in the temporal evolution of isotopic signature recorded in both systems.  
424 Remarkably, as mentioned above, “closed”-system (Rayleigh-type) model predicts positive  
425  $\Delta^{33}\text{S}$  and negative  $\Delta^{36}\text{S}$  signatures which, again, were not observed here, possibly pointing  
426 towards yet unknown specific S fractionation mechanisms.

427 The second remarkable feature observed for the Green River Fm and Lake Dziani Dzaha was  
428 the strong depletion in heavy S isotopes of  $\text{S}_{\text{org}}$  relative to sulfides (by -25 to -30 ‰ for  $^{34}\text{S}$ ).  
429 Such an isotopic shift has been previously reported in some studies of the Green River Fm,  
430 but the values were not discussed further than the fact that they were out of range compared to  
431 usual marine and euxinic environments (Mauger et al., 1973; Tuttle and Goldhaber, 1993).  
432 Interestingly, a recent compound-specific  $^{34}\text{S}/^{32}\text{S}$  analysis of organic matter from the Cariaco  
433 Basin showed a *ca.* 10 ‰ depletion of several OSC (*e.g.*, triterpenoid thianes, and acyclic  
434 isoprenoid thiophenes and thiolanes) relative to pyrite and to total extractable and residual  $\text{S}_{\text{org}}$   
435 (Raven et al., 2015). The authors suggested that total  $\text{S}_{\text{org}}$  likely contains a mixture of OSC  
436 with distinct S-isotopic compositions formed by different sulfurization pathways (reversible  
437 vs irreversible sulfurization processes). Shawar et al. (2018) further suggested that  $^{34}\text{S}$ -  
438 depletion of OSC relative to pyrite could be the result of competitive reactions between iron,  
439 sulfur and organic matter, in particular in iron-limited environments. Under these specific  
440 conditions, contrary to the ‘open’ marine systems described above, organic compounds might  
441 react with reduced sulfur species at the earliest stage of burial more efficiently than iron, thus  
442 recording the  $\delta^{34}\text{S}$  signature of reactive sulfides whereas the formation of iron sulfides might  
443 be delayed due to complexation or sorption of iron by the organic matter (Fig. 8b). S-isotopic  
444 shifts between  $\text{S}_{\text{org}}$  and mineral sulfides might thus result from a predominant kinetic isotope

445 effects occurring during the fast sulfurization of organic matter by different pathways that  
446 remain to be characterized.

447

#### 448 4. CONCLUSIONS

449 We validated a new stepwise chemical procedure for the quantitative recovery and multi-  
450 isotope ( $^{33}\text{S}$ ,  $^{34}\text{S}$  and  $^{36}\text{S}$ ) analysis of  $\text{S}_{\text{org}}$  present in both solvent-extractable (bitumen) and  
451 residual (kerogens) organic matter. This method is further compatible with the analysis of  
452 different inorganic S species ( $\text{S}^0$ , sulfates and sulfides) in the same samples. The most  
453 distinguishing feature of this procedure is the use of NaOCl as an oxidative agent for the  
454 degradation of organic matter and release of  $\text{S}_{\text{org}}$  as recoverable sulfates. The efficiency of this  
455 analytical oxidation step was demonstrated with geological samples of various age and S-  
456 content (contemporary anoxic sediment, source rocks and oil), noticeably showing that it does  
457 not introduce any artificial fractionation of  $\text{S}_{\text{org}}$  multi-isotopes. This method can be used either  
458 for the determination by EA-IRMS of the S-content and  $\delta^{34}\text{S}$  of different S-pools recovered as  
459  $\text{Ag}_2\text{S}$  powders, or for the high-precision multi-isotope analysis of these  $\text{Ag}_2\text{S}$  powders by  
460 IRMS ( $\delta^{33}\text{S}$ ,  $\delta^{34}\text{S}$  and  $\delta^{36}\text{S}$  from  $\text{SF}_6$ ) or MC-ICPMS ( $\delta^{33}\text{S}$ ,  $\delta^{34}\text{S}$ ).

461 The application of this S multi-pool approach to samples from the Mahogany zone of the  
462 Green River Fm and the contemporaneous Lake Dziani Dzaha revealed striking and similar  
463 features of their S isotope composition, including highly-enriched mineral sulfides (with  
464 values of  $\delta^{34}\text{S}$  around +35‰), and pools of  $\text{S}_{\text{org}}$  depleted in  $^{34}\text{S}$  by *ca.* -27 ‰ relative to  
465 sulfides. This depletion contrasts with the typical (+5/+10 ‰) enrichment in  $^{34}\text{S}$  of  $\text{S}_{\text{org}}$   
466 relative to sulfides observed in marine sediments and confirmed in the present study with a  
467 sample from the Monterey Fm (for which we report a +4.9 ‰ enrichment in  $^{34}\text{S}$  of  $\text{S}_{\text{org}}$   
468 relative to sulfides). Such uncommon S isotopic characteristics probably point to fast

469 sulfurization of organic matter (with a kinetically controlled S fractionation) from  $^{34}\text{S}$ -  
470 enriched sulfides/sulfates, leading to a strong  $^{34}\text{S}_{\text{org}}$  depletion.

471

## 472 **ACKNOWLEDGEMENTS**

473 The authors would like to thank Bryan Killingsworth (IPGP), Amaury Bouyon (IPGP),  
474 Laetitia Guibourdenche (IPGP) and François Fourel (LEHNA) for their precious suggestions  
475 and assistance in this work, as well as Alex L. Sessions and an anonymous reviewer who  
476 helped to improve the manuscript with their constructive feedback.

477 This study was funded by TOTAL E&P, the Lyon Institute of Origins (LabEx LIO) and the  
478 French CNRS interdisciplinary research program (ISOTOP 2018-2019, MULTISORG  
479 project).

480

## 481 **REFERENCES**

482 Adam, P., Schmid, J.C., Mycke, B., Strazielle, C., Connan, J., Huc, A., Riva, A., Albrecht, P.,  
483 1993. Structural investigation of nonpolar sulfur cross-linked macromolecules in  
484 petroleum. *Geochim. Cosmochim. Acta* 57, 3395–3419.

485 Albalat, E., Telouk, P., Balter, V., Fujii, T., Miossec, P., Zoulim, F., Puisieux, A., 2016.  
486 Sulfur isotope analysis by MC-ICP-MS and application to small medical samples. *J.*  
487 *Anal. Atom.Spectrom.* 31, 1002–1011.

488 Amrani, A., 2014. Organosulfur compounds: Molecular and isotopic evolution from biota to  
489 oil and gas. *Annu. Rev. Earth Planet. Sci.* 42, 733–768.

490 Amrani, A., Deev, A., Sessions, A.L., Tang, Y., Adkins, J.F., Hill, R.J., Moldowan, J.M.,  
491 Wei, Z., 2012. The sulfur-isotopic compositions of benzothiophenes and  
492 dibenzothiophenes as a proxy for thermochemical sulfate reduction. *Geochim.*

493           Cosmochim. Acta 84, 152–164.

494   Amrani, A., Sessions, A.L., Adkins, J.F., 2009. Compound-specific  $\delta^{34}\text{S}$  analysis of volatile  
495           organics by coupled GC/multicollector-ICPMS. *Anal. Chem.* 81, 9027–9034.

496   Anderson, T.F., Pratt, L.M., 1995. Isotopic evidence for the origin of organic sulfur and  
497           elemental sulfur in marine sediments, in: Vairavamurthy, M., Schoonen, M.A.A. (Eds.),  
498           *Geochemical Transformations of Sedimentary Sulfur*. pp. 378–396.

499   Arnold, G.L., Brunner, B., Müller, I.A., Røy, H., 2014. Modern applications for a total sulfur  
500           reduction distillation method - what's old is new again. *Geochem. Trans.* 15, 1–12.

501   Au Yang, D., Landais, G., Assayag, N., Widory, D., Cartigny, P., 2016. Improved analysis of  
502           micro- and nanomole-scale sulfur multi- isotope compositions by gas source isotope ratio  
503           mass spectrometry. *Rapid Commun. Mass Sp.* 30, 897–907.

504   Bigeleisen, J., Mayer, M.G., 1947. Calculation of equilibrium constants for isotopic exchange  
505           reactions. *J. Chem. Phys.* 15, 261–267.

506   Blumer, M., 1957. Removal of elemental sulfur from hydrocarbon fractions. *Anal. Chem.* 29,  
507           1039–1041.

508   Bradley, W.H., 1964. Geology of Green River Formation and associated Eocene rocks in  
509           south- western Wyoming and adjacent parts of Colorado and Utah. *Geol. Surv. Prof.*  
510           Pap. 496-A, 81–84.

511   Canfield, D.E., 2001. Biogeochemistry of sulfur isotopes. *Rev. Mineral. Geochem.* 43, 607–  
512           636.

513   Canfield, D.E., Boudreau, B.P., Mucci, A., Gundersen, J.K., 1998. The early diagenetic  
514           formation of organic sulfur in the sediments of Mangrove Lake, Bermuda. *Geochim.*

515       Cosmochim. Acta 62, 767–781.

516   Canfield, D.E., Raiswell, R., Westrich, J.T., Reaves, C.M., Berner, R.A., 1986. The use of  
517       chromium reduction in the analysis of reduced inorganic sulfur in sediments and shales.  
518       Chem. Geol. 54, 249–254.

519   Eardley, A.J., 1963. Oil seeps at Rozel Point. Utah Geol. Mineral. Surv. Spec. Stud. 5.

520   Eschka, A., 1874. Estimation of sulphur in coal and coke. J. Chem. Soc. 27, 1007.

521   Farquhar, J., Bao, H., Thiemens, M., 2000. Atmospheric influence of Earth's earliest sulfur  
522       cycle. Science 289, 756–758.

523   Farquhar, J., Johnston, D.T., Wing, B.A., Habicht, K.S., Canfield, D.E., Airieau, S.,  
524       Thiemens, M.H., 2003. Multiple sulphur isotopic interpretations of biosynthetic  
525       pathways: implications for biological signatures in the sulphur isotope record.  
526       Geobiology 1, 27–36.

527   Farquhar, J., Wing, B.A., 2003. Multiple sulfur isotopes and the evolution of the atmosphere.  
528       Earth Planet. Sc. Lett. 213, 1–13.

529   Farquhar, J., Johnston, D.T., Wing, B.A., 2007. Implications of conservation of mass effects  
530       on mass-dependent isotope fractionations: Influence of network structure on sulfur  
531       isotope phase space of dissimilatory sulfate reduction. Geochim. Cosmochim. Acta 71,  
532       5862-5875.

533   Forrest, J., Newman, L., 1977. Silver-110 Microgram sulfate analysis for the short time  
534       resolution of ambient levels of sulfur aerosol. Anal. Chem. 49, 1579–1584.

535   Fossing, H., Jorgensen, B.B., 1989. Measurement of bacterial sulfate reduction in sediments:  
536       Evaluation of a single-step chromium reduction method. Biogeochemistry 8, 205–222.

537 Fourel F., Martineau F., Seris M. and Lécuyer C. 2014. Simultaneous N, C, S stable isotope  
538 analyses using new purge and trap technology. *Rapid Commun. Mass Sp.* 28, 2587–  
539 2594.

540 Giesemann, A., Jager, H., Norman, A.L., Krouse, H.R., Brand, W.A., 1994. On-line sulfur-  
541 isotope determination using an elemental analyzer coupled to a mass spectrometer. *Anal.*  
542 *Chem.* 66, 2816–2819.

543 Gröger, J., Franke, J., Hamer, K., Schulz, H.D., 2009. Quantitative recovery of elemental  
544 sulfur and improved selectivity in a chromium-reducible sulfur distillation. *Geostand.*  
545 *Geoanal. Res.* 33, 17–27.

546 Hulston, J. R., Thode, H. G., 1965. Cosmic ray produced  $^{36}\text{S}$  and  $^{33}\text{S}$  in metallic phase of  
547 iron meteorites: *J. Geophys. Res.* 70, 4435–4442.

548 Johnston, D.T., 2011. Multiple sulfur isotopes and the evolution of Earth ' s surface sulfur  
549 cycle. *Earth-Sci. Rev.* 106, 161–183.

550 Johnston, D.T., Farquhar, J., Wing, B.A., Kaufman, A.J., Canfield, D.E., Habicht, K.S., 2005.  
551 Multiple sulfur isotope fractionations in biological systems : a case study with sulfate  
552 reducers and sulfur disproportionators. *Am. J. Sci.* 305, 645–660.

553 Kutuzov, I., Rosenberg, Y.O., Bishop, A., Amrani, A., 2018. The Origin of Organic Sulphur  
554 Compounds and Their Impact on the Paleoenvironmental Record. In: H. Wilkes (ed.),  
555 Hydrocarbons, Oils and Lipids: Diversity, Origin, Chemistry and Fate. *Handbook of*  
556 *Hydrocarbon and Lipid Microbiology.* Springer, Cham.

557 Labidi, J., Farquhar, J., Alexander, C.M.O'D., Eldridge, D.L., Oduro, H., 2017. Mass  
558 independent sulfur isotope signatures in CMs : Implications for sulfur chemistry in the  
559 early solar system. *Geochim. Cosmochim. Acta* 196, 326-350.



- 560 Leboulanger, C., Agogu , H., Bernard, C., Bouvy, M., Carr , C., Cellamare, M., Duval, C.,  
561 Fouilland, E., Got, P., Intertaglia, L., Lavergne, C., Le Floc'h, E., Roques, C., Sarazin,  
562 G., 2017. Microbial diversity and cyanobacterial production in Dziani Dzaha crater lake,  
563 a unique tropical thalassohaline environment. *PLoS One* 12, 1–28.
- 564 Li, W., Cho, E.H., 2005. Coal desulfurization with sodium hypochlorite. *Energ. Fuel* 19, 499–  
565 507.
- 566 Luo, G., Richoz, S., van de Schootbrugge, B., Algeo, J., Xie, S., Ono, S., Summons, R.E.,  
567 2018. Multiple sulfur-isotopic evidence for a shallowly stratified ocean following the  
568 Triassic-Jurassic boundary mass-extinction. *Geochim. Cosmochim. Acta* 231, 73–87.
- 569 Mauger, R.L., Kayser, R.B., Gwynn, W., 1973. A Sulfur isotopic study of Uinta Basin  
570 hydrocarbons. *Utah Geol. Mineral. Surv. Spec. Ser.* 41, 19.
- 571 Milesi, V.P., Debure, M., Marty, N.C.M., Capano, M., Jezequel, D., Steefel, C.I., Rouchon,  
572 V., Alb ric, P., Bard, E., Sarazin, G., Guyot, F., Virgone, A., Gaucher, E.C., Ader, M.,  
573 2020. Early Diagenesis of Lacustrine Carbonates in Volcanic Settings: The Role of  
574 Magmatic CO<sub>2</sub> (Lake Dziani Dzaha, Mayotte, Indian Ocean). *ACS Earth Space Chem.*,  
575 4, 363-378.
- 576 Oduro, H., Kamyshny, A., Guo, W., Farquhar, J., 2011. Multiple sulfur isotope analysis of  
577 volatile organic sulfur compounds and their sulfonium precursors in coastal marine  
578 environments. *Mar. Chem.* 124, 78–89.
- 579 Ono, S., Shanks, W.C., Rouxel, O.J., Rumble, D., 2007. S-33 constraints on the seawater  
580 sulfate contribution in modern seafloor hydrothermal vent sulfides. *Geochim.*  
581 *Cosmochim. Acta* 71, 1170–1182.
- 582 Ono, S., Wing, B., Johnston, D., Farquhar, J., Rumble, D., 2006a. Mass-dependent

583 fractionation of quadruple stable sulfur isotope system as a new tracer of sulfur  
584 biogeochemical cycles. *Geochim. Cosmochim. Acta* 70, 2238–2252.

585 Ono, S., Wing, B., Rumble, D., Farquhar, J., 2006b. High precision analysis of all four stable  
586 isotopes of sulfur ( $^{32}\text{S}$ ,  $^{33}\text{S}$ ,  $^{34}\text{S}$  and  $^{36}\text{S}$ ) at nanomole levels using a laser fluorination  
587 isotope-ratio-monitoring gas chromatography-mass spectrometry. *Chem. Geol.* 225, 30-  
588 39.

589 Orr, W.L., 1986. Kerogen/asphaltene/sulfur relationships in sulfur-rich Monterey oils. *Org.*  
590 *Geochem.* 10, 499–516.

591 Paris, G., Sessions, A.L., Subhas, A.V., Adkins, J.F., 2013. MC-ICP-MS measurement of  $\delta^{34}\text{S}$   
592 and  $\Delta^{33}\text{S}$  in small amounts of dissolved sulfate. *Chem. Geol.* 345, 50-61.

593 Passier, H.F., Middelburg, J.J., de Lange, G.J., Böttcher, M.E., 1999. Modes of sapropel  
594 formation in the eastern Mediterranean : some constraints based on pyrite properties.  
595 *Marine Geology* 153, 199-219.

596 Pepkowitz, L.P., Shirley, E.L., 1950. Microdetection of Sulfur. *Anal. Chem.* 23, 1709–1710.

597 Philippot, P., Van Zuilen, M., Lepot, K., Thomazo, C., Farquhar, J., Van Kranendonk, M.J.,  
598 2007. Early Archaean Microorganisms Preferred Elemental Sulfur, Not Sulfate. *Science*  
599 317, 1534-1537.

600 Raven, M.R., Adkins, J.F., Werne, J.P., Lyons, T.W., Sessions, A.L., 2015. Sulfur isotopic  
601 composition of individual organic compounds from Cariaco Basin sediments. *Org.*  
602 *Geochem.* 80, 53–59.

603 Raven, M.R., Fike, D.A., Gomes, M.L., Webb, S.M., Bradley, A.S., 2018. Organic carbon  
604 burial during OAE2 driven by changes in the locus of organic matter sulfurization. *Nat.*

605 Commun. 9, 3409.

606 Raven, M.R., Sessions, A.L., Adkins, J.F., Thunell, R.C., 2016a. Rapid organic matter  
607 sulfurization in sinking particles from the Cariaco Basin water column. *Geochim.*  
608 *Cosmochim. Acta* 190, 175–190.

609 Raven, M.R., Sessions, A.L., Fischer, W.W., Adkins, J.F., 2016b. Sedimentary pyrite  $\delta^{34}\text{S}$   
610 differs from porewater sulfide in Santa Barbara Basin: Proposed role of organic sulfur.  
611 *Geochim. Cosmochim. Acta* 186, 120–134.

612 Rees, C.E., 1978. Sulphur isotope measurements using  $\text{SO}_2$  and  $\text{SF}_6$ . *Geochim. Cosmochim.*  
613 *Acta* 42, 383–389.

614 Sansjofre, P., Cartigny, P., Trindade, R.I.F., Nogueira, A.C.R., Agrinier, P., Ader, M., 2016.  
615 Multiple sulfur isotope evidence for massive oceanic sulfate depletion in the aftermath of  
616 Snowball Earth. *Nat. Commun.* 7, 12192.

617 Selvig, W.A., Fieldner, A.C., 1927. Sulfur in coal and coke: Check determinations by the  
618 Eschka, bomb-washing and sodium peroxide fusion methods. *Ind. Eng. Chem.* 19, 729–  
619 733.

620 Shawar, L., Halevy, I., Said-Ahmad, W., Feinstein, S., Boyko, V., Kamyshny, A., Amrani, A.,  
621 2018. Dynamics of pyrite formation and organic matter sulfurization in organic-rich  
622 carbonate sediments. *Geochim. Cosmochim. Acta* 241, 219–239.

623 Shawar, L., Said-Ahmad, W., Ellis, G.S., Amrani, A., 2020. Sulfur isotope composition  
624 of individual compounds in immature organic-rich rocks and possible geochemical  
625 implications. *Geochim. Cosmochim. Acta*, doi: 10.1016/j.gca.2020.01.034.

626 Siedenbergh, K., Strauss, H., Podlaha, O., van den Boorn, S., 2018. Multiple sulfur isotopes

627 ( $\delta^{34}\text{S}$ ,  $\Delta^{33}\text{S}$ ) of organic sulfur and pyrite from Late Cretaceous to Early Eocene oil  
628 shales in Jordan. *Org. Geochem.* 125, 29–40.

629 Sinninghe Damsté, J.S., Rijpstra, W.I.C., Kock-Van Dalen, A.C., De Leeuw, J.W., Schenck,  
630 P.A., 1989. Quenching of labile functionalised lipids by inorganic sulphur species:  
631 Evidence for the formation of sedimentary organic sulphur compounds at the early stages  
632 of diagenesis. *Geochim. Cosmochim. Acta* 53, 1343–1355.

633 Smith, M.E., Carroll, A.R., 2015. *Stratigraphy and Paleolimnology of the Green River*  
634 *Formation, Western USA*. Springer, Dordrecht.

635 Thode, H.G., Monster, J., Dunford, H.B., 1961. Sulphur isotope geochemistry. *Geochim.*  
636 *Cosmochim. Acta* 25, 159–174.

637 Thode, H.G., Monster, J., Dunford, H.B., 1958. Sulphur isotope abundances in petroleum and  
638 associated materials. *Bulletin Am. Assoc. Pet. Geol.* 42, 2619–2641.

639 Thode, H.G., Rees, C.E., 1971. Measurement of sulphur concentrations and the isotope ratios  
640  $^{33}\text{S}/^{32}\text{S}$ ,  $^{34}\text{S}/^{32}\text{S}$  and  $^{36}\text{S}/^{32}\text{S}$  in Apollo 12 samples. *Earth Planet. Sci. Lett.* 12, 434–  
641 438.

642 Thomassot, E., Cartigny, P., Harris, J.W., Lorand, J.P., Rollion-Bard, C., Chaussidon, M.,  
643 2009. Metasomatic diamond growth: A multi-isotope study ( $^{13}\text{C}$ ,  $^{15}\text{N}$ ,  $^{33}\text{S}$ ,  $^{34}\text{S}$ ) of  
644 sulphide inclusions and their host diamonds from Jwaneng (Botswana). *Earth Planet. Sci.*  
645 *Lett.* 282, 79–90.

646 Tissot, B.P., Welte, D.H., 1984. *Petroleum Formation and Occurrence*, Second Edi. ed.  
647 Springer-Verlag.

648 Tuttle, M.L., 1991. *Geochemical, biogeochemical, and sedimentological studies of the Green*

649 River Formation, Wyoming, Utah, and Colorado. USGS Numbered Ser. 1973-A-G, 200.

650 Tuttle, M.L., Goldhaber, M.B., 1993. Sedimentary sulfur geochemistry of the Paleogene  
651 Green River Formation, western USA: Implications for interpreting depositional and  
652 diagenetic processes in saline alkaline lakes. *Geochim. Cosmochim. Acta* 57, 3023–  
653 3039.

654 Wang, YG, Wei, X.Y., Yan, H.L., Liu, F.J., Li, P., Zong, Z.M., 2014. Sequential oxidation of  
655 Jincheng No. 15 anthracite with aqueous sodium hypochlorite. *Fuel Process. Technol.*  
656 125, 182-189.

657 Werne, J.P., Lyons, T.W., Hollander, D.J., Formolo, M.J., Sinninghe Damsté, J.S., 2003.  
658 Reduced sulfur in euxinic sediments of the Cariaco Basin: sulfur isotope constraints on  
659 organic sulfur formation. *Chem. Geol.* 195, 159–179.

660 Werne, J.P., Lyons, T.W., Hollander, D.J., Schouten, S., Hopmans, E.C., Sinninghe Damsté,  
661 J.S., 2008. Investigating pathways of diagenetic organic matter sulfurization using  
662 compound-specific sulfur isotope analysis. *Geochim. Cosmochim. Acta* 72, 3489–3502.

663 Whitehouse, M.J., 2012. Multiple sulfur isotope determination by SIMS: Evaluation of  
664 reference sulfides for  $\Delta^{33}\text{S}$  with observations and a case study on the determination of  
665  $\Delta^{36}\text{S}$ . *Geostand. Geoanal. Res.* 37, 19–33.

666 Young, E.D., Galy, A., Nagahara, H., 2002. Kinetic and equilibrium mass-dependent isotope  
667 fractionation laws in nature and their geochemical and cosmochemical significance.  
668 *Geochim. Cosmochim. Acta* 66, 1095–1104.

669 Zaback, D.A., Pratt, L.M., 1992. Isotopic composition and speciation of sulfur in the Miocene  
670 Monterey Formation : Reevaluation of sulfur reactions during early diagenesis in marine  
671 environments. *Geochim. Cosmochim. Acta* 56, 763–774.

672 Zinke, J., Reijmer, J.J.G., Thomassin, B.A., 2003. Systems tracts sedimentology in the lagoon  
673 of Mayotte associated with the Holocene transgression. *Sed. Geol.* 160, 57-784.

**Table 1** Methods previously used for studying the  $^{34}\text{S}$  composition of organic and mineral S. For further details about STRIP and  $\text{CrCl}_2$  distillations, see 3.2. \* Studies in which  $^{33}\text{S}$  and/or  $^{36}\text{S}$  were also measured. n/i: not investigated.

**Table 2** Origin, nature and use of samples. O = oxidation tests (Figs. 3 and 4), N = Raney nickel tests (Table 3), W = complete workflow procedure (triplicate analyses, Table 4), L = comparison with literature data and biogeochemical interpretation.

**Table 3** Comparison of  $\text{S}_{\text{org}}$  contents (mg/g of dry sediment) released with the Raney nickel method (Oduro et al., 2011) and the new method from selected samples. TLE = solvent-soluble organic matter.

**Table 4** S content (mg/g of dry sediment) and multiple-isotope composition (‰ vs CDT) of the different S pools from the investigated samples. n/d: non determined or excluded value, due to either a lack of material (under limit of detection) or mass spectrometry issues/contaminations. \*The 4<sup>th</sup> replicate of Lake Dziani Dzaha was sampled in a different part of the core than the three others. It was therefore not used in the mass balance calculations. TLE  $\text{S}_{\text{org}}$  = solvent-soluble  $\text{S}_{\text{org}}$  and Kerogen  $\text{S}_{\text{org}}$  = solvent-insoluble  $\text{S}_{\text{org}}$ .

Table 1

Study	Sample type	Total S	Sulfides	Sulfates	S <sup>0</sup>	S <sub>org</sub>
Thode et al. (1958)	Oil	Calculated	Bubbled out	Centrifuged out	n/i	Br <sub>2</sub> , HNO <sub>3</sub> oxidation to sulfates, STRIP distillation, SO <sub>2</sub> IRMS
	Bulk sediment	n/i	Br <sub>2</sub> , HNO <sub>3</sub> oxidation to sulfates, STRIP distillation, SO <sub>2</sub> IRMS	Dissolution + precipitation, STRIP distillation, SO <sub>2</sub> IRMS	n/i	n/i
Mauger et al. (1973)	Organic extract from tar sand	n/i	n/i	n/i	n/i	Br <sub>2</sub> oxidation + STRIP distillation, SO <sub>2</sub> IRMS
Orr (1986)	Solvent-extracted sediment	Calculated	HNO <sub>3</sub> oxidation to sulfates, EA-IRMS	n/i	n/i	Parr bomb oxidation to sulfates, EA-IRMS
	Oil/organic extract from sediment					Parr bomb oxidation to sulfates, EA-IRMS
Zaback and Pratt (1992)	Solvent-extracted sediment	Calculated	CrCl <sub>2</sub> distillation, SO <sub>2</sub> IRMS	Dissolution + precipitation, SO <sub>2</sub> IRMS		
	Organic extract from the sediment	Calculated			Combustion, SO <sub>2</sub> IRMS	Parr bomb oxidation, SO <sub>2</sub> IRMS
Tuttle and Goldhaber (1993)	Bulk sediment	Calculated	CrCl <sub>2</sub> distillation, SO <sub>2</sub> IRMS analysis	SO <sub>2</sub> IRMS analysis	n/i	Eschka oxidation, SO <sub>2</sub> IRMS
Werne et al. (2008, 2003)	Solvent-extracted sediment	EA-IRMS on bulk sediment	CrCl <sub>2</sub> distillation, EA-IRMS	EA-IRMS on pore water precipitates	n/i	EA-IRMS
	Organic extract from the sediment		CrCl <sub>2</sub> distillation, EA-IRMS		n/i	EA-IRMS + compound-specific EA-IRMS
Amrani et al. (2012, 2009)	Oil/Organosulfur standard	EA-IRMS	n/i	n/i	n/i	Compound-specific MC-ICPMS
Oduro et al. (2011)	Solvent-extracted sediment	Calculated	CrCl <sub>2</sub> distillation, SF <sub>6</sub> IRMS*	STRIP distillation, SF <sub>6</sub> IRMS* on pore water precipitates		n/i
	Organic extract from the sediment	Calculated			CrCl <sub>2</sub> distillation, SF <sub>6</sub> IRMS*	Raney Ni desulfurization + CrCl <sub>2</sub> distillation, SF <sub>6</sub> IRMS*
Raven et al. (2018, 2016a, 2016b, 2015)	Solvent-extracted sediment	Calculated	HNO <sub>3</sub> oxidation to sulfates, ion chromatography, ICPMS/EA-IRMS	Dissolution + precipitation, ion chromatography, ICPMS/EA-IRMS		n/i
	Organic extract from the sediment	Calculated			Oxidation, ion chromatography, ICPMS/EA-IRMS	H <sub>2</sub> O <sub>2</sub> oxidation, ion chromatography, ICPMS/EA-IRMS + compound-specific MC-ICPMS
Siedenberg et al. (2018)	Solvent-extracted sediment	n/i	CrCl <sub>2</sub> distillation, SF <sub>6</sub> IRMS*	n/i		Eschka powder oxidation + STRIP distillation, SF <sub>6</sub> IRMS*
	Organic extract from the sediment	n/i			n/i	Eschka powder oxidation + STRIP distillation, SF <sub>6</sub> IRMS*
This study	Solvent-extracted sediment	EA-IRMS on bulk sediment	CrCl <sub>2</sub> distillation, SF <sub>6</sub> IRMS*	STRIP distillation, SF <sub>6</sub> IRMS*		NaHClO oxidation + STRIP distillation, SF <sub>6</sub> IRMS*
	Oil/Organic extracts from the sediment				CrCl <sub>2</sub> distillation, SF <sub>6</sub> IRMS*	NaHClO oxidation + STRIP distillation, SF <sub>6</sub> IRMS*



Table 2

	<i>Sample source</i>	<i>Sediment type</i>	<i>Age</i>	<i>TOC (%)</i>	<i>Use</i>
Lake Dziani Dzaha (Mayotte, Indian Ocean)	Sub-superficial sediment	Euxinic lake sediment	Modern (0-1 kyr after Milesi et al., 2020)	9.2 ±0.3	O + N + W + L
Green River Fm (UT, USA)	Outcrop & core sediments	Microbialite	Eocene (ca. 50 Myr)	31.8 ±0.4	O + N + W + L
Monterey Fm (CA, USA)	Outcrop sediment	Shale	Miocene (5-17 Myr)	7.1 ±0.5	O + W + L
Rozel Point oil (UT, USA)	Oil seep	Crude oil	Tertiary	49.3 ±0.5	O + N + W
Limagne Basin (Massif Central, France)	Outcrop sediment	Microbialite	Oligo-Miocene (5-34 Myr)	13.4 ±0.1	N

Table 3

	<i>New method</i>	<i>Raney nickel</i>
Lake Dziani Dzaha TLE	0.33 ± 0.05 (n=3)	0.047 ± 0.01 (n=3)
Green River Fm TLE	2.32 ± 0.02 (n=2)	0.11 ± 0.05 (n=2)
Limagne Basin kerogen	1.11 ± 0.03 (n=2)	0.32 ± 0.02 (n=2)
Rozel Point oil	91.78 ± 1.05 (n=3)	0.46 ± 0.12 (n=2)

Table 4

<i>Sample</i>	<i>Pool</i>	<i>Replicate</i>	<i>S quantity</i>	$\delta^{34}S$	$\delta^{33}S$	$\delta^{36}S$	$\Delta^{33}S$	$\Delta^{36}S$
Monterey Fm	Sulfides	1	4.759	2.666	1.465	5.67	0.028	-0.53
		2	5.015	2.251	1.252	4.89	0.029	-0.51
		3	4.416	3.454	1.874	7.16	0.032	-0.53
	Sulfates	1	0.560	4.739	2.573	9.22	0.070	-0.89
		2	0.534	5.868	3.126	11.47	0.043	-0.790
		3	0.642	7.370	3.920	14.29	0.065	-0.84
	S <sup>0</sup>	1	< 0.005	n/d	n/d	n/d	n/d	n/d
		2	< 0.005	n/d	n/d	n/d	n/d	n/d
		3	< 0.005	n/d	n/d	n/d	n/d	n/d
	Kerogen S <sub>org</sub>	1	3.428	8.768	4.623	17.20	0.051	-0.60
		2	3.462	8.691	4.586	16.97	0.055	-0.68
		3	3.829	8.732	4.615	17.02	0.062	-0.71
	TLE S <sub>org</sub>	1	0.339	5.871	3.145	11.62	0.061	-0.65
		2	0.269	n/d	n/d	n/d	n/d	n/d
		3	0.285	6.151	3.295	11.86	0.067	-0.94
Rozel Point	Sulfides	1	< 0.005	n/d	n/d	n/d	n/d	n/d
		2	< 0.005	n/d	n/d	n/d	n/d	n/d
		3	< 0.005	n/d	n/d	n/d	n/d	n/d
	Sulfates	1	< 0.005	n/d	n/d	n/d	n/d	n/d
		2	< 0.005	n/d	n/d	n/d	n/d	n/d
		3	< 0.005	n/d	n/d	n/d	n/d	n/d
	S <sup>0</sup>	1	< 0.005	n/d	n/d	n/d	n/d	n/d
		2	< 0.005	n/d	n/d	n/d	n/d	n/d
		3	< 0.005	n/d	n/d	n/d	n/d	n/d
	Kerogen S <sub>org</sub>	1	< 0.005	n/d	n/d	n/d	n/d	n/d
		2	< 0.005	n/d	n/d	n/d	n/d	n/d
		3	< 0.005	n/d	n/d	n/d	n/d	n/d
	TLE S <sub>org</sub>	1	92.836	-6.165	-3.034	-11.58	0.081	-1.07
		2	90.728	-6.025	-2.963	-11.33	0.079	-1.08
		3	91.765	-5.960	-2.924	-11.18	0.085	-1.06
Lake Dziani	Sulfides	1	2.363	35.143	18.027	69.07	0.014	0.37
		2	2.485	35.651	18.278	69.86	0.008	0.17
		3	2.382	35.528	18.216	70.14	0.009	0.67
		4*	2.522	37.126	19.027	72.71	0.011	0.14
	Sulfates	1	0.353	n/d	n/d	n/d	n/d	n/d
		2	0.409	n/d	n/d	n/d	n/d	n/d
		3	0.484	n/d	n/d	n/d	n/d	n/d
		4*	0.387	33.216	17.077	64.86	0.040	-0.08
	S <sup>0</sup>	1	0.647	n/d	n/d	n/d	n/d	n/d
		2	0.632	n/d	n/d	n/d	n/d	n/d
		3	0.709	n/d	n/d	n/d	n/d	n/d
		4*	0.556	39.583	20.245	77.67	-0.014	0.29
	Kerogen S <sub>org</sub>	1	3.768	6.701	3.491	13.82	-0.019	-0.06
		2	3.478	5.933	3.119	12.05	0.003	-0.35
		3	3.812	6.781	3.546	14.05	-0.006	0.02
4*		3.603	8.228	4.290	16.69	-0.004	-0.09	
TLE S <sub>org</sub>	1	0.300	9.613	5.001	19.64	-0.003	0.21	
	2	0.385	10.169	5.277	20.80	-0.012	0.30	
	3	0.319	10.548	5.474	21.56	-0.010	0.34	
	4*	0.256	9.070	4.705	18.17	-0.020	-0.21	
Green Riv. Fm	Sulfides	1	10.002	34.714	17.733	68.98	-0.062	1.08
		2	9.960	35.337	18.050	69.98	-0.061	0.88
		3	9.303	35.266	17.999	69.78	-0.076	0.82
	Sulfates	1	0.905	27.832	14.248	n/d	-0.055	n/d
		2	< 0.005	n/d	n/d	n/d	n/d	n/d
		3	0.924	25.349	12.971	n/d	-0.070	n/d
	S <sup>0</sup>	1	< 0.005	n/d	n/d	n/d	n/d	n/d
		2	< 0.005	n/d	n/d	n/d	n/d	n/d
		3	< 0.005	n/d	n/d	n/d	n/d	n/d
	Kerogen S <sub>org</sub>	1	3.821	9.002	4.644	n/d	-0.047	n/d
		2	4.013	8.690	4.497	17.78	-0.034	0.11
		3	3.527	10.069	5.209	n/d	-0.029	n/d
	TLE S <sub>org</sub>	1	2.302	5.848	3.062	12.03	-0.010	-0.22
		2	< 0.005	n/d	n/d	n/d	n/d	n/d
		3	2.331	5.718	3.001	12.98	-0.005	0.94

**Fig. 1.** Proposed workflow for the sequential recovery of organic and mineral S from sediments/oils as Ag<sub>2</sub>S powders, prior to their fluorination and S multi-isotope analysis.

**Fig. 2.** Experimental setup used for S distillation; **a**, sample with gentle reflux, **b**, reducing solution (CrCl<sub>2</sub>/STRIP), **c**, nitrogen flush, **d**, water acid-trap, **e**, silver nitrate sulfur-trap.

**Fig. 3.** Organic carbon content (**a**) and S<sub>org</sub> recovery (**b**) of selected samples along 48 hours of NaOCl oxidation at 60°C.

**Fig. 4.** δ<sup>34</sup>S of recovered S<sub>org</sub> as a function of NaOCl oxidation time at 60°C.

**Fig. 5.** Comparison of S mass balances between bulk EA-IRMS and multi-pool SF<sub>6</sub>-IRMS (new method) analyses; **a**, TS content calculated from Ag<sub>2</sub>S weighing as a function of EA-IRMS bulk evaluation; **b**, bulk δ<sup>34</sup>S calculated with mass-balance equations from multi-pool SF<sub>6</sub>-IRMS analyses, as a function of EA-IRMS bulk evaluation. Error bars show the standard deviation between triplicate analyses.

**Fig. 6.** Multi-isotope data from the samples of this study; open diamonds, sulfides, open circles, sulfates, open triangles, S<sup>0</sup>, black diamonds, soluble S<sub>org</sub>, black circles, insoluble S<sub>org</sub>. **a** and **c** show mass-dependent fractionation of all S-isotopes. **b** and **d** show the interest of the Δ notation to enhance the variability between samples.

**Fig. 7.** Comparison between δ<sup>34</sup>S in sedimentary sulfides and kerogens. Data for the Green River Fm is from Tuttle & Goldhaber (1993), data for the Monterey Fm is from Zaback and Pratt (1992). The expected range for marine sediments is extrapolated after Orr (1986).

**Fig. 8.** Two possible models for S geochemistry and organic matter sulfurization during sediment deposition and diagenesis. **A** shows S fractionation associated with organic matter sulfurization in the anoxic part of the sediments in ‘open’ marine environments such as the Monterey Fm. The inflow S derives from marine sulfates. **B** shows S fractionation associated with organic matter sulfurization in a partially sulfidic stratified water column with a high H<sub>2</sub>S/sulfates ratio from a ‘closed’ system such as some Green River Fm members and Lake Dziani Dzaha. The inflow S derives from enriched sulfates resulting from the Rayleigh fractionation of marine sulfates in a closed system (as suggested by Tuttle, 1991). MSR = Microbial Sulfate Reduction.

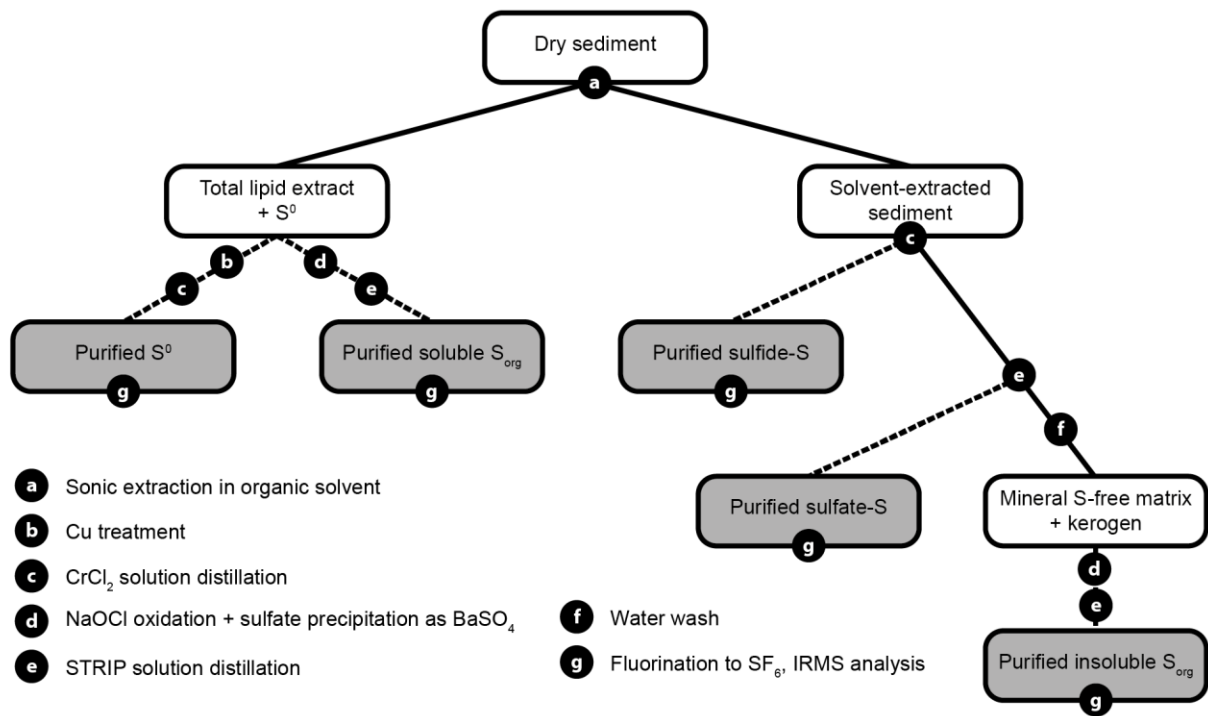


Figure 1

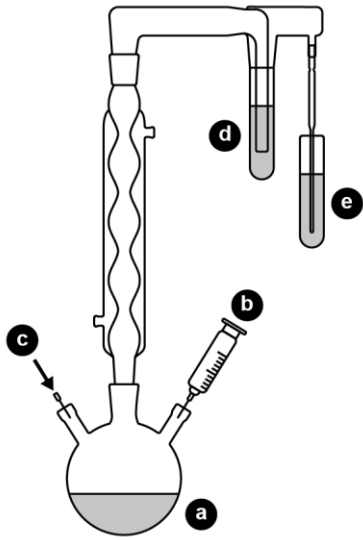


Figure 2

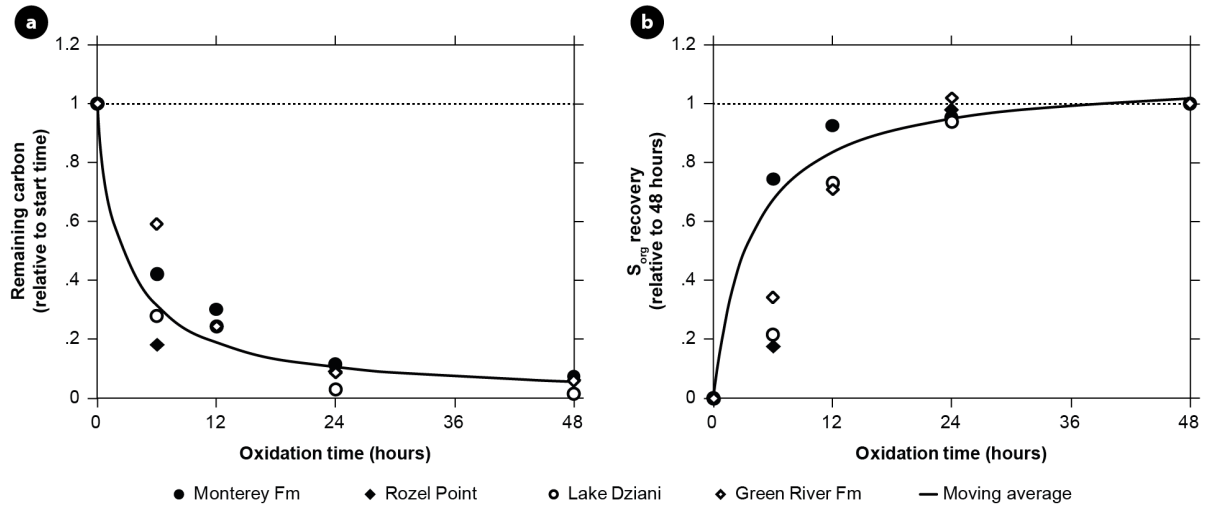


Figure 3

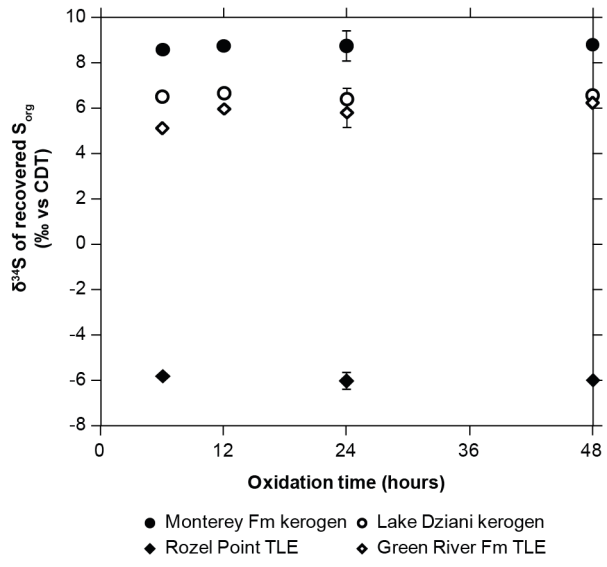


Figure 4



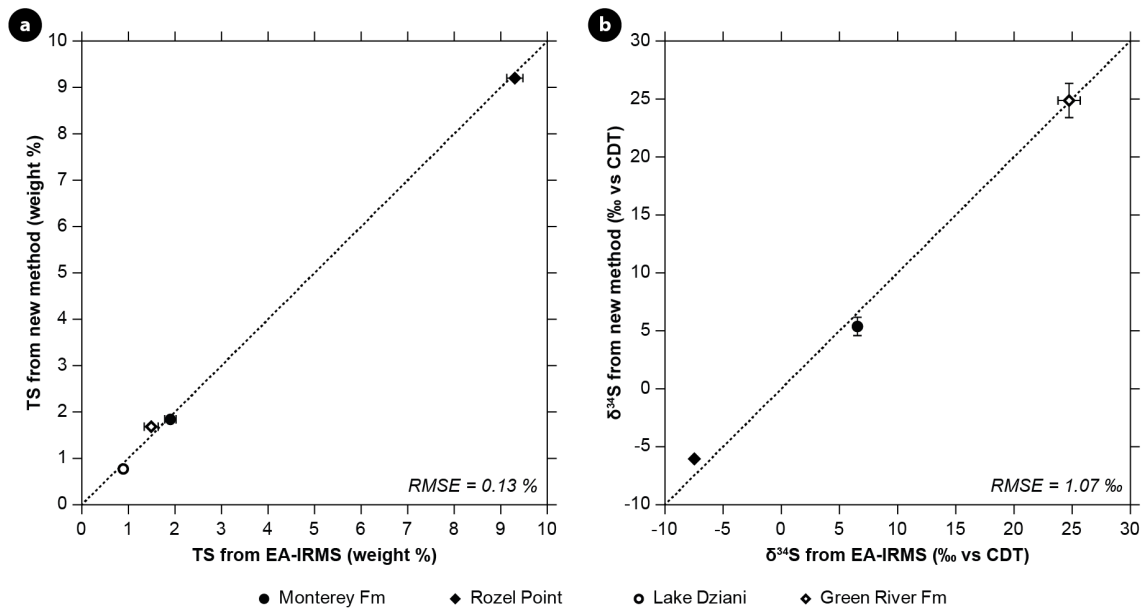


Figure 5

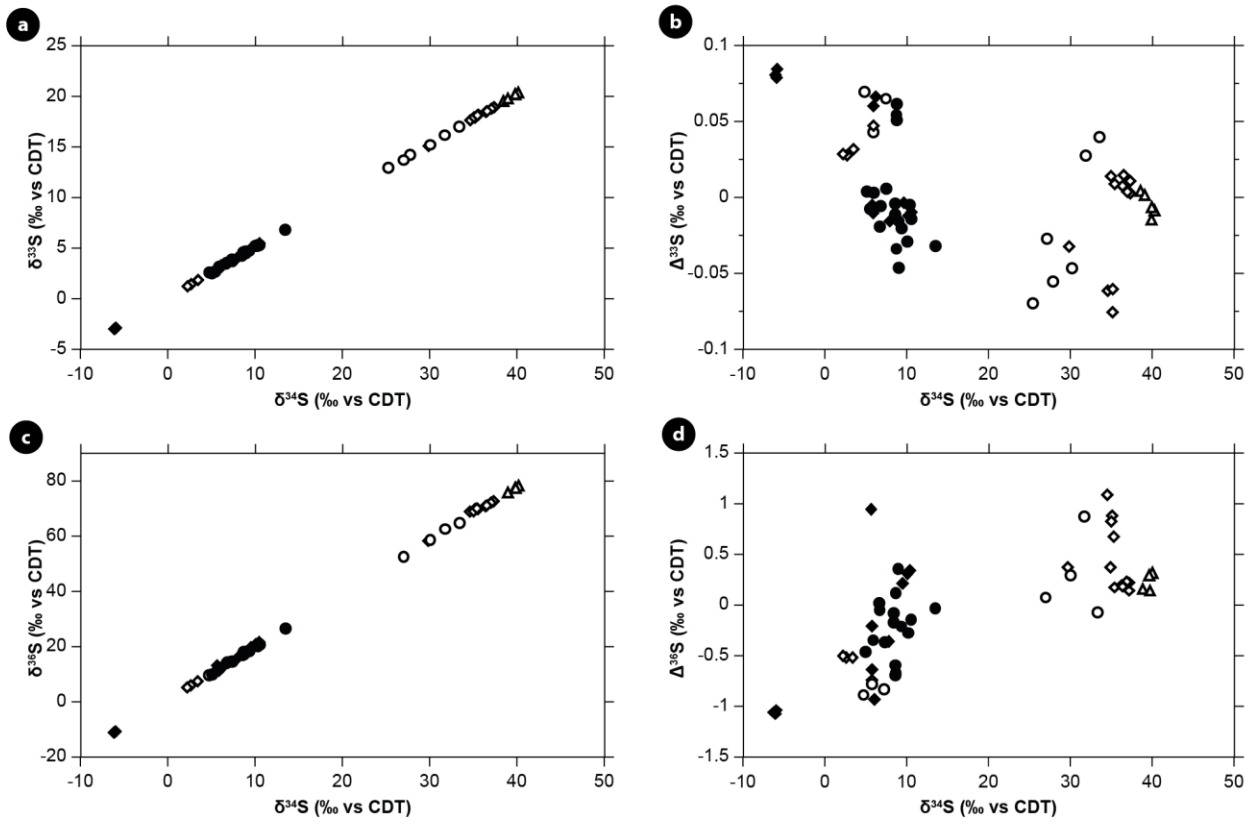


Figure 6

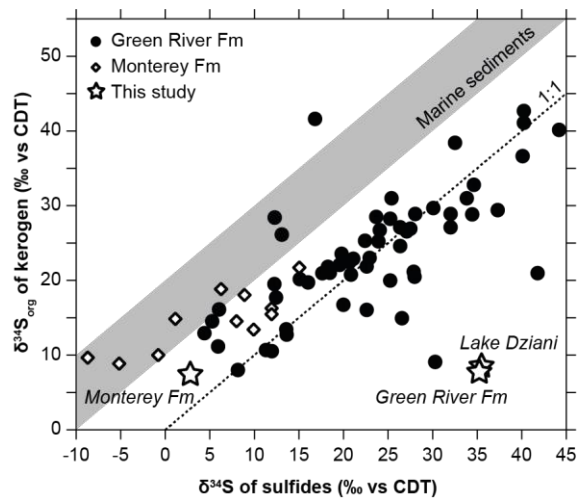


Figure 7

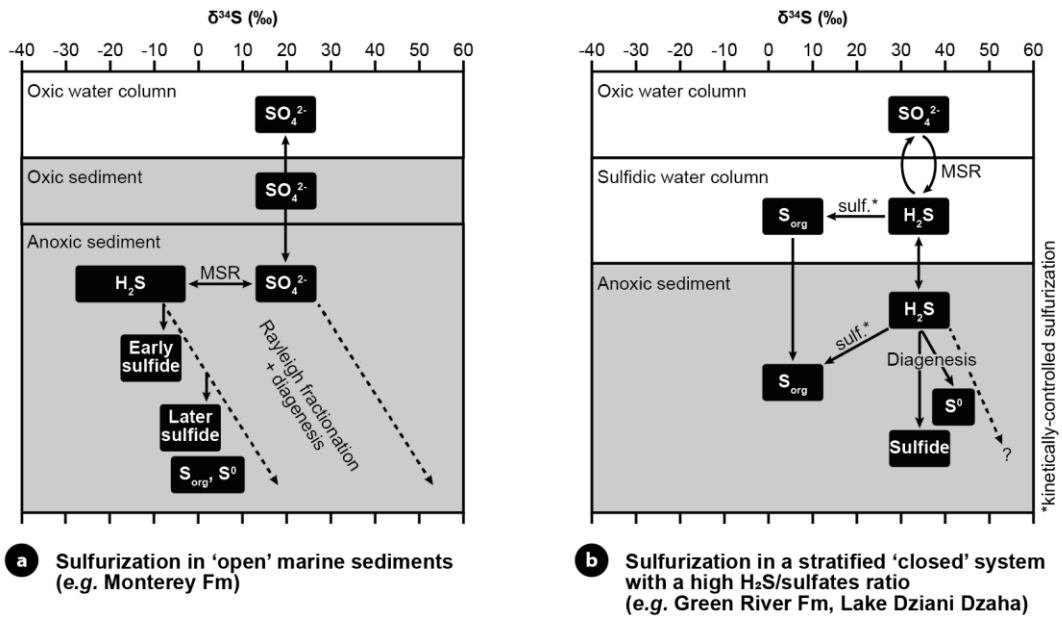


Figure 8